Journal of the Taiwan Institute of Chemical Engineers 000 (2015) 1–10

Contents lists available at ScienceDirect

Journal of the Taiwan Institute of Chemical Engineers

journal homepage: www.elsevier.com/locate/jtice

Acidity and catalytic performance of Yb-doped SO_4^{2-}/Zr in comparison with SO_4^{2-}/Zr catalysts synthesized *via* different preparatory conditions for biodiesel production

Yahaya Muhammad Sani [a,b], Peter Adeniyi Alaba [a], Aisha Olatope Raji-Yahya [b], A.R. Abdul Aziz [a], Wan Mohd Ashri Wan Daud [a,*]

[a] Department of Chemical Engineering, University of Malaya, 50603 Kuala Lumpur, Malaysia
[b] Department of Chemical Engineering, Ahmadu Bello University, 870001 Zaria, Nigeria

ARTICLE INFO

Article history:
Received 8 April 2015
Revised 15 June 2015
Accepted 15 July 2015
Available online xxx

Keywords:
Catalyst preparation
Bifunctional catalyst
Acid activation
Solid acid catalyst
Biodiesel

ABSTRACT

Highly efficient, robust and mesoporous sulfated zirconia, SZ catalysts were prepared by co-precipitation and incipient-wetness routes with sufficient and in-excess acid. The study investigated the effect of pH, precursor type, and concentration, on SZ and compared their acidity and performance with ytterbium-doped SZ toward transesterification. N_2 sorption, elemental analysis, XRD, and ammonia temperature-programmed desorption (NH_3-TPD) revealed the properties of the catalytic materials. The specific surface area increases independently of the presence of Ti up to 60.33 m^2/g, with increasing pH while pore size of the tetragonal crystallites decreases from 37.04 to 6.83 nm. Soaking the material in sufficient 0.5-M H_2SO_4 produced 37.04 nm S_{BET} in contrast to 21.21 nm from soaking in excess. Double sulfation ensured sulfate incorporation while moderate precursor amounts enhanced activity of the materials. Interestingly, despite low specific surface area, which was due to short aging period, large mesoporosity, high amount, and dispersion of active sites on Yb-doped SZ, SZr-Ti-Yb-500-4/s ensured remarkable activity. The catalyst converted *ca.* 99% of used frying oil containing *ca.* 48 wt. % FFA. Consequently, this highlights the prospect of producing biodiesel at lower cost especially with current dwindling price of crude oil.

1. Introduction

The potency of public concern in the 21st century forces decision makers to enact policies not primarily based on science and technology. Concerns such as environmental impacts and socioeconomical challenges help to shape public opinion toward new demands which require novel catalytic solutions [1,2]. Inherent with these new challenges are the potentials for greater efficiency and sustainability of such systems [3]. Moreover, the searches for newer solutions have led experts to explore in details, the attributes of different materials, systems and devices [4]. One key task is in achieving phase-homogeneous solids with uniform morphological and chemical properties. This challenge is a fundamental prerequisite to any rational catalyst design. Further, the current dwindling price of crude oil is an indication that catalysis needs extensive experimentation to give biofuel the needed competitive edge. Consequently, it is necessary to devise catalytic processes with *ca.* 100% yields. These will help to establish the potentials of catalysts as well as ensure the prominence of biofuels such as biodiesel. Despite these challenges, last century witnessed catalysis as the major backbone for most industrial processes such as petrochemistry (especially, petroleum catalytic refining) and bulk chemistry. Incidentally, the high activity of sulfated zirconia (SZ) attracted substantial attention for converting triglycerides (TGs) into biodiesel at moderate to high temperatures. SZ is the subject of numerous reports since its discovery in 1979 [5]. Considering the numerous reports available in the open literature, it is plausible to assert that SZ has attained a 'state-of-the-art' status. Further, most reports considered SZ as superacids because of their catalytic activity in simultaneously esterifying free fatty acids (FFA) and transesterifying triglycerides (TG) from high-FFA containing feedstocks into biodiesel.

However, despite numerous encouraging results, some aspects of SZ catalytic reactivity and physicochemical properties remain debatable. Some authors [6–8] argue that despite the presence of sulfate anions, the hydroxyl groups on the SZ surface are less acidic than the bridged hydroxyls in zeolites. They further claimed that besides Lewis sites, the surface of zirconia contains basic sites in the form of coordinated unsaturated oxygen atoms. They attributed this

* Corresponding author. Tel.: +601 1263 76195, +60 3796 75297; fax: +60 3796 75319.
E-mail addresses: ymsani@siswa.um.edu.my (Y.M. Sani), adeniyipee@live.com (P.A. Alaba), raji.aisha@gmail.com (A.O. Raji-Yahya), ashri@um.edu.my (W.M.A.W. Daud).

http://dx.doi.org/10.1016/j.jtice.2015.07.016
1876-1070/

rationale by viewing the interaction between zirconia and H_2SO_4 as acid–base reaction. Contrarily, proponents [9–11] to its acidity provided evidences that showed super acidity of SZ contains two types of acid sites. A strong acidic site (24 μmol) with up to 31.2 kcal/mol strength and a weaker site (52 μmol) having a strength of 25.8 kcal/mol. The latter explains the claim by the opponents to the acidity of SZ. This is because 25.8 kcal/mol is lower than 34 kcal/mol and 41 kcal/mol that represent the acidity of HY and HZSM-5 respectively. The latter acidity explains the observation reported by the opposing authors. However, these conflicting reports are not surprising because heterogeneity and site accessibility of solid acid catalysts render direct measurement elusive. Moreover, acidity of SZ is sensitive to preparatory conditions and preparation method employed [1].

Two decades ago, a detailed report by [12] evidenced the negligible effect that sulfation procedure has on the final SZ product. Despite this and the extensive attention on the factors affecting the acidity of SZ, there is no information from open literature regarding biodiesel production over SZ doped with ytterbium. Consequently, the present contribution aims to demonstrate the superior acidity and catalytic activity of SZ doped with ytterbium over SZ catalysts prepared by varying preparative procedures. To achieve this, the study evaluated how slight changes during incipient wetness and co-precipitation methods, and sulfate dispersion on SZ affect its acidity and performance in biodiesel production. The report aims at providing insight to the arduous task of making biodiesel economically competitive via transesterifying UFO containing 48 wt. % FFA. It is instructive to highlight the significance of employing UFO especially with current dwindling price of crude oil. Rather than dump the waste material into landfills, UFO simultaneously eliminates the food-for-fuel competition [13] and reduces the cost of biodiesel production [14]. The cooking process causes the vegetable oil, TGs, to breakdown to form, DGs, MGs, and free fatty acids (FFAs).

2. Materials and method

Sigma-Aldrich supplied all the reagents for this study. To ensure better comparative analyses, the study synthesized three different batches of catalytic materials. These were: (a) catalysts prepared via incipient method, (b) ytterbium doped catalysts, and (c) materials synthesized via co-precipitation. The required amount of ZrO_2 (5 μm, 99%) was soaked in excess 0.5-M H_2SO_4 (≥ 98%) and stirred for 120 min. Fritted glass filtered the resultant solution prior to drying of the solid for 20 h in open-air inside a fume cupboard; and at 130 °C for 16 h in an oven. Calcination was for 4 h at 500 °C. The acronym SZr-T-t/x represents the synthesized materials. Where *T* denotes calcination temperature, *t* signifies time, while *x* denotes sufficient soaking(s), soaking in excess (*e*), or aging period (days). These preparatory variables were varied (see Table 1) to elucidate their effects on acidity and activity.

Further, homogeneous co-precipitation was the route employed for synthesizing the second batch of catalytic materials. Aqueous solutions of 1:2 wt. % of $ZrOCl_2.8H_2O$ (≥ 99.5%) and TiO_2 (*ReagentPlus*®, ≥ 99%, 4.26 g/mL at 25 °C) were thoroughly mixed with urea. The mixture was heated at 95 °C under vigorous stirring for 12 h. Repeated washing of the precipitate with distilled water after filtering ensured negligible Cl^- concentration. The solid was initially oven-dried for 12 h at 120 °C, and then stored in dry N_2 atmosphere. Immersing 6 g of Zr–Ti composite in 0.5-M H_2SO_4 facilitated sulfation, while water bath evaporated the excess moisture. The resultant solid was oven-dried at 130 °C for 16 h and calcined at 500 °C for 4 h. This sample was designated as SZr-Ti-500-4/e. To investigate the effect that transition metal has on activity, Ytterbium (III) nitrate pentahydrate, $Yb(NO_3)_3.5H_2O$ (crystals and lumps; 99.9% trace metals basis) was added to the third batch of catalysts. NH_4OH (≥ 99.99% trace metals basis; 28% NH_3 in H_2O) was added to aqueous mixture of Zr and Ti and stirred for 2 h. The resultant solid was oven-dried at 110 °C for 24 h and ground into powder. A thorough mixing of the samples with aqueous 0.5-M H_2SO_4 incorporated sulfate ions, while heating at 110 °C for 12 h prior to calcination at 500 °C for 4 h ensured stability on the materials. The material was designated SZr-Ti-Yb-500-4/s.

The third batch of catalytic materials was prepared according to a modified procedure previously documented by [15]. Distilled water and continuous stirring for 5 min, dissolved the required amount of $ZrOCl_2.8H_2O$ to 0.34-M concentration. Adding urea in drop-wise manner to the required pH, precipitated the active species from the solution. While adding 0.5 M $(NH_4)_2SO_4$ produced a gel-like acidic solution. This was aged for 1–14 days in closed polyethylene (PE) bottles at 90 °C. The solution underwent filtration after cooling to room temperature, and subsequent washing with excess distilled water (6 times, each with 200 mL). Calcination of the solid in air at 500 °C for 5 h followed drying in open-air for 20 h, and heating at 90 °C for 4 h in a fume cupboard. These samples were designated as SZr-500-5/7. To evaluate the effect of strong acid sites, a portion of SZr-500-4/7, designated SZr-500-4/7R underwent a re-sulfation procedure again. After drying, kneading, mixing with 0.5 M-H_2SO_4 for 2 h, filtering through fritted glass, and drying at 130 °C for 16 h, the solids were calcined at 500 °C for 4 h. The procedure was repeated for sample SZr-500-5/14 except that required amount of $ZrOCl_2.8H_2O$ was dissolved in distilled water before adding urea to a pH value of 5. Similarly, the procedure was repeated for SZr/500-5/10 except required amount of $ZrO(NO_3)_2.xH_2O$ was dissolved in 400 mL distilled water before adding urea to pH value of 3 and mixing with required amount of $Al(NO_3).9H_2O$. Continuous stirring under 210 rpm at 50 °C for 2 h aided homogeneity. Adding ammonia solution and stirring for 40 min preceded aging at room temperature for 10 days. Subsequently, after filtering, drying in fume cupboard at 90 °C for 24 h, and calcining at 500 °C for 5 h, the catalysts were stored in airtight vials inside a desiccator. All catalysts and experimental runs were prepared in replicates to ensure repeatability.

Table 1
Variable parameters employed for synthesizing mesoporous sulfated zirconia.

Sample ID	0.5-M H_2SO_4	pH	Aging (h)
SZr-500-4/e	excess	–	2
SZr-500-4/s	sufficient	–	2
SZr-500-1/e	excess	–	0.25
SZr-Ti-500-4/e	excess	–	0.25
SZr-Ti-500-4/s	sufficient	–	0.25
SZr-Ti-Yb-500-4/s	0.323	–	2
SZr-500-5/7	0.034	1.25	168
SZr-500-5/7R	0.039	2	168
SZr-500-5/14	0.071	5	336
SZr-500-5/10	0.038	4	240

2.1. Catalyst characterization

Analyzing isolated catalytic materials, precursors, or intermediates facilitates circumventing the high complexities of catalytic systems. It provides important information regarding the reaction mechanism and structure/activity relationships of the catalyst. Further, *ex situ* approach also enables the researcher to work with simplified systems under predefined conditions. Consequently, surface morphology and topology were analyzed with field emission scanning electron microscopy (FE-SEM) FEI QUANTA™ 450 FEG type 2033/14 (Czech Republic) unit with 30 kV accelerating voltage. An energy dispersive X-ray spectrometer (EDX) from the same unit revealed the surface elemental composition of the catalysts. XRD and BET analyses elucidated the structural and textural properties of the catalysts. Phillips X'pert diffractometer (The Netherlands) with CuKα radiation (λ = 1.54056 Å) at a scanning speed of 0.05°s^{-1} within 2θ

Please cite this article as: Y.M. Sani et al., Acidity and catalytic performance of Yb-doped SO_4^{2-}/Zr in comparison with SO_4^{2-}/Zr catalysts synthesized *via* different preparatory conditions for biodiesel production, Journal of the Taiwan Institute of Chemical Engineers (2015), http://dx.doi.org/10.1016/j.jtice.2015.07.016

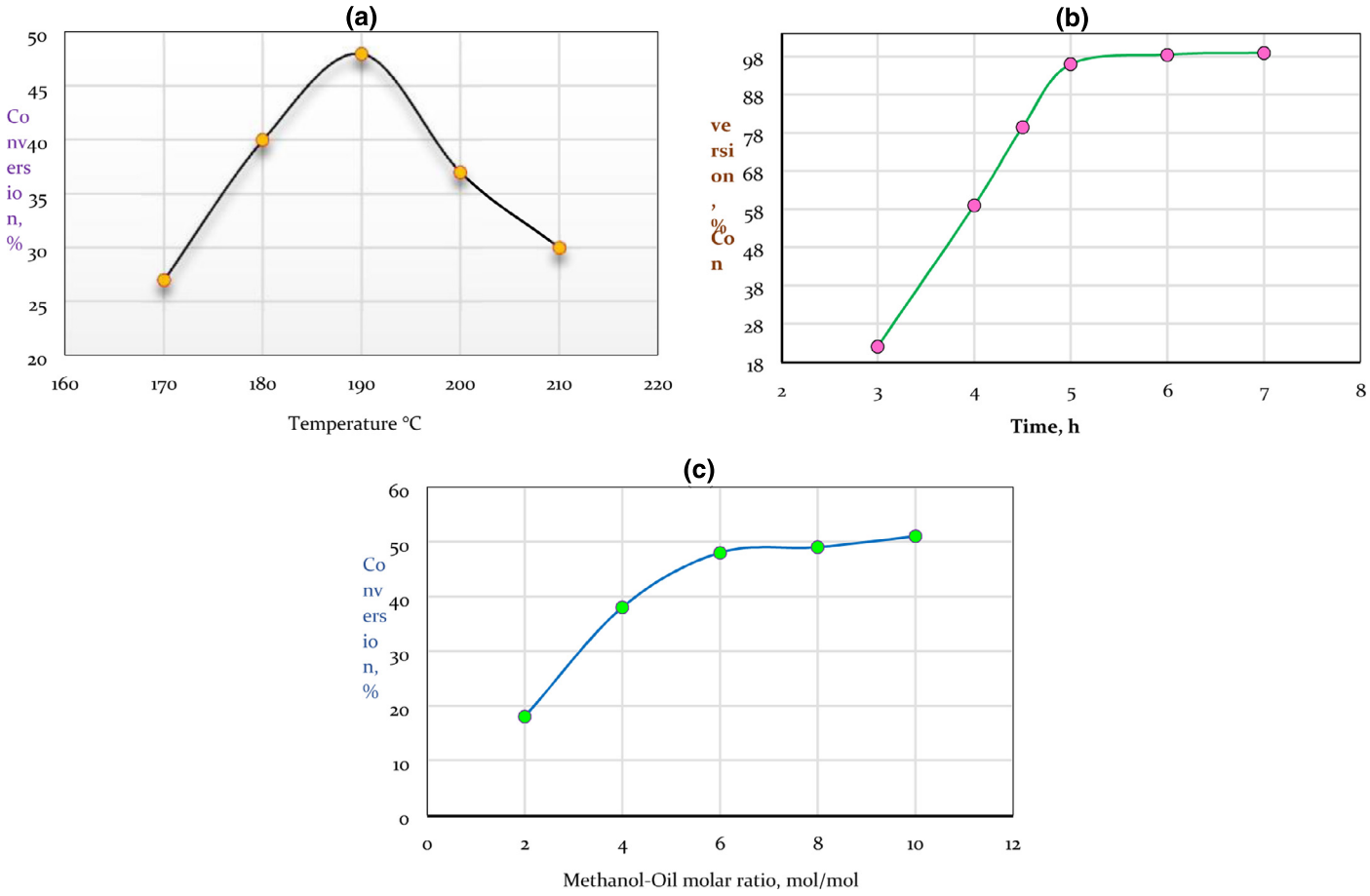

Fig. 1. Preliminary optimization of reaction variables: (a) temperature, (b) time and, (c) methanol-to-oil molar ratio.

range of 5–70° at 40 mA and 40 kV analyzed the XRD patterns. A Micromeritics TriStar II (USA) with accelerated surface area porosity (ASAP) 3020 at –196.15 °C was used to determine the specific surface area of the catalytic materials using liquid nitrogen. Degassing the catalysts at 120 °C for 3 h under a vacuum eliminated any physisorbed volatiles and impurities. Rapid (scan speed 3 velocities, 2.2–20 kHz) identification and quantification of the catalysts was performed with a Bruker Fourier transform infrared (FT-IR) Tensor 27 IR (Germany). The apparatus has a spectral range of 7500–370 cm^{-1} with more than 1 cm^{-1} apodized resolution and a standard KBr beam splitter. Ammonia temperature programmed desorption (NH_3-TPD) by AutoChem 2920 (Micromeritics) evaluated the acidic profiles on the catalysts. To ascertain the exact amount of gas consumed during the experiment, the equipment was calibrated by 10% NH_3 in He before the analysis. After placing 0.10 g in a quartz U-tube, N_2 flow (50 mL/min) at 110 °C for 1 h degassed the synthesized material. After cooling to 60 °C, the samples were saturated with NH_3 by the (20 mL/min) flow of 10% NH_3 in He for 40 min. N_2 gas flowing at 50 mL/min for 30 min over catalyst purged the physisorbed NH_3. Raising the temperature from 60 to 700 °C with a ramp of 10 °C/min under N_2, flowing at 50 mL/min revealed the TPD profile. TCD detector revealed the amount of NH_3 consumed which determines the Brønsted and Lewis acid sites in the catalyst.

2.2. Production of fatty acid methyl esters

Heating the catalysts at 150 °C for 1 h before the reaction evacuates adsorbed water and other volatiles. With the aid of catalyst, 23.40 mL of used frying oil, UFO (866 g/mol) was esterified and transesterified simultaneously with methanol at 100–220 °C, while the pressure varied according to the process temperature inside the reactor. The reactors employed for conducting the reaction were a 100 mL autoclaves (250 °C, 100 bar) supplied by AmAr Equipment Pvt., Ltd. (Mumbai). Constant stirring ensured contact between the catalyst and the reaction mixture. A reflux condenser attached to the autoclave maintained the temperature during the reaction. Preliminary optimization (Fig. 1) showed that a 6:1 methanol-to-oil molar ratio and 2 wt. % catalyst loading are optimal reaction conditions. However, this study employed a molar ration of 5:1 because the difference in conversion was minimal. This minimizes the use of resource, energy, and cost. Simple decanting and centrifugation recovered the FAME at the end of the 5 h reaction time.

The study employed GC–MS (Serial # CN10946045; Model 7890A; US), and EN 14103:2003 (E) analytical method in determining methyl ester contents with 100-mg neat mixture (Supelco® No. 18919) containing 37 components (C_4 to C_{24} FAMEs; 2–4% relative concentration) as reference standard. This was dissolved in 99% heptane at 0.01–0.10% (w/v) concentration. Then, 1 mL hexane placed in vials with screw caps having PTFE-faced septa dissolves an accurately weighed 10 mg sample, prior to the addition of 10 μL of 2 N KOH in methanol. After vortex for 30 s, and centrifugation, 1 μL of the supernatant was transferred into TSP micro vial. The GC analyzer has the following working conditions: DB 23 column (L = 0.30 mm × ID = 0.32 mm × 0.25 μm film thickness of 5% diphenyl, 95% dimethyl polysiloxane) and methyl heptadecanoate, C_{17} (99% minimum purity; 14 min retention time) as the internal standard; 210 °C injection temperature and helium as carrier gas. Eq. 1 facilitated the determination of the ester content (C), expressed

Please cite this article as: Y.M. Sani et al., Acidity and catalytic performance of Yb-doped SO_4^{2-}/Zr in comparison with SO_4^{2-}/Zr catalysts synthesized *via* different preparatory conditions for biodiesel production, Journal of the Taiwan Institute of Chemical Engineers (2015), http://dx.doi.org/10.1016/j.jtice.2015.07.016

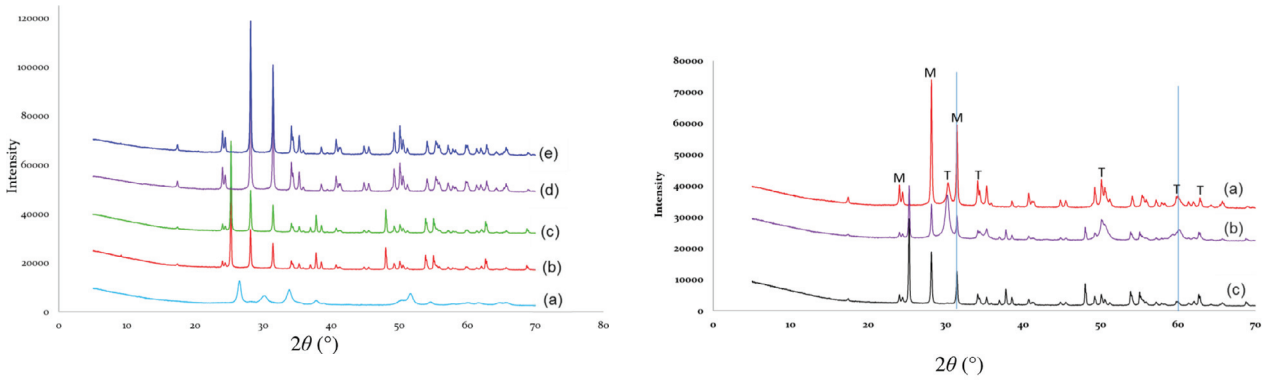

Fig. 2. (A) X-ray diffraction patterns for (a) SZr-Ti-Yb-500-4/s, (b) SZr-500/e, (c) SZr-500-4/s, (d) SZr-Ti-500-4/e and (e) SZr-Ti-500-4/s. (B) X-ray diffraction patterns for (a) SZr-500-5/7, (b) SZr-500-5/14 and (c) SZr-500-5/10.

Table 2
Textural properties and acidity of synthesized sulfated zirconia.

Sample ID	Surface area (m^2/g)	Pore vol. (cm^3/g)	Pore size (nm)	Acidity (x 10^{-3} mmol/g)
SZr-500-4/e	5.30 ± 0.5	0.020	21.21	20 ± 0.02
SZr-500-4/s	3.43 ± 0.2	0.017	37.04	40 ± 0.02
SZr-500-1/e	3.84 ± 0.3	0.018	20.35	10 ± 0.01
SZr-Ti-500-4/e	8.12 ± 1.3	0.043	24.98	50 ± 0.03
SZr-Ti-500-4/s	8.33 ± 1.4	0.047	28.52	70 ± 0.03
SZr-Ti-Yb-500-4/s	60.33 ± 2.3	0.323	21.38	330 ± 0.05
SZr-500-5/7	7.69 ± 1.4	0.034	21.44	80 ± 0.03
SZr-500-5/7R	9.05 ± 1.3	0.039	20.27	40 ± 0.03
SZr-500-5/14	41.22 ± 1.9	0.071	6.83	280 ± 0.04
SZr-500-5/10	15.05 ± 1.7	0.038	9.65	70 ± 0.03

as a mass fraction in percentage.

$$C = \frac{\left(\sum^{A}\right) - A_{E1}}{A_{E1}} \times \frac{C_{E1} \times V_{E1}}{m} \times 100\% \quad (1)$$

Where:

ΣA is the total peak area from the methyl ester in C_{14} to that in $C_{24:1}$;
A_{E1} is the peak area corresponding to methyl heptadecanoate;
C_{E1} is the concentration of the methyl heptadecanoate, in mg/mL;
V_{E1} is the volume of the methyl heptadecanoate, in mL;
m is the mass of the sample, in mg.

3. Results and discussion

3.1. X-ray diffraction analysis

The XRD diffractograms (Figs. 2a and b) of the synthesized SZ catalysts revealed a tetragonal-monoclinic phase transition. The XRD patterns also show the significant impact of calcination temperature and precursor concentration on the crystal phase and crystallite size. Further, tetragonal phase exhibited more prominent characteristic peak areas than its monoclinic phase counterpart. In addition, the intensity of the peaks reflected both adsorption and amount of phase in the synthesized materials. Usually tetragonal phase transition occurs at above 1170 °C. However, according to [16,17], SZ precipitation preparation method produces monoclinic-tetragonal phase transformation of zirconia at lower temperature.

Therefore, the low temperature employed during synthesis in this study facilitated the transition of monoclinic phase to tetragonal phase which retards crystallization of zirconia support [18,19]. Furthermore, the higher surface energy of the monoclinic phase compared to that of tetragonal phase ensures the metastable tetragonal phase transformation [17]. All the XRD patterns displayed presence of monoclinic and tetragonal phases except SZr-Ti-Yb-500-4/s (Fig. 2b). This is despite the variance in the preparatory methods and precursor types utilized. The amount and chemical composition of the latter material was different from all other samples. This explains the differences observed from the crystallographic structures. Expectedly, the tetragonal phase (111) reflection at $2\theta = 31.02$ XRD patterns of the SZ broadens with higher pH. However, the (111) reflection of the monoclinic phase at $2\theta = 28.18°$ especially for the sample prepared at higher pH indicated unstable tetragonal phase because probably the crystallite size were not small enough [20].

Conversely, SZ prepared at higher pH exhibited lower monoclinic phases. Further, SZr-Ti-Yb-500-4/s that was synthesized with repeated addition of ammonium hydroxide exhibited lower crystalline structures with major anatase titania. The sample however, displayed similar pore size distribution to SZr-500-4/s but with 20 fold higher S_{BET} (Table 2). The two materials were both soaked for 2 h in sufficient H_2SO_4. Consequently, the difference in sintering process, which causes higher S_{BET} (Table 1), confirmed the phase transformation exhibited by the XRD pattern of SZr-Ti-Yb-500-4/s. Interestingly, the materials processed is sufficient, but under longer soaking period exhibited higher acidity and pore diameter. For instance, entries 2 and 3 (Table 1) showed higher pore sizes and active site dispersion than those soaked in excess. This informed the preparation of SZr-Ti-Yb-500-4/s, which despite its lower width/height SZ peak ratio and crystallite size exhibited the highest S_{BET} and acidity. Similarly, the sample in entry 9, displayed higher S_{BET} and acidity than the one in entry 10 (Table 1). Therefore, it is plausible to assert that higher SO_4^{2-} concentration in SZr-Ti-Yb-500-4/s, facilitated the retardation of tetragonal phase transforming into monoclinic phase.

It is also evident from the peak intensities that reflectance of adsorption and amount of phase in the mixture of SZr-Ti-Yb-500-4/s were lower than for the other materials. SZr-Ti-500-4/e, SZr-Ti-500-4/s and SZr-500-5/7 displayed zirconia predominantly in monoclinic phase with little tetragonal phase with respect to intensity. The monoclinic phase had highest intensity at $2\theta = 28.16°$ (61.21%) while that of the tetragonal is at $2\theta = 50.09°$ (13.27%). In contrast, SZr-500-4/e,

Please cite this article as: Y.M. Sani et al., Acidity and catalytic performance of Yb-doped SO_4^{2-}/Zr in comparison with SO_4^{2-}/Zr catalysts synthesized *via* different preparatory conditions for biodiesel production, Journal of the Taiwan Institute of Chemical Engineers (2015), http://dx.doi.org/10.1016/j.jtice.2015.07.016

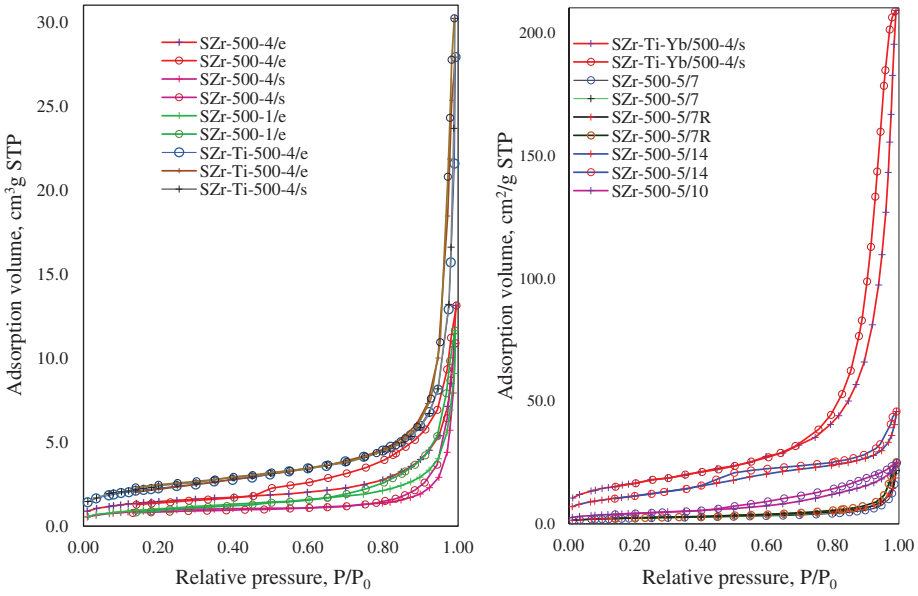

Fig. 3. N_2 adsorption–desorption isotherms of mesoporous SZ synthesized from different conditions.

SZr-500-4/s, SZr-500-5/14 and SZr-500-5/10 exhibited zirconia predominantly in tetragonal phase with little monoclinic phase with respect to intensity. The tetragonal phase has the highest intensity at $2\theta = 30.19°$ (81.74%) while that of the monoclinic was at $2\theta = 28.17°$ (64.43%). Figs. (2a and b) also highlight the effect that slight modification in catalyst preparatory conditions has on the morphology of the material. These morphological changes could be favorable or detrimental to the catalytic activity of the catalysts. Such alterations affected the domain sizes and lattice strains (*i.e.*, the contribution from crystalline sizes and strains) displayed by the peaks. The peaks also revealed the concentrations of active metal in the different modified catalysts. The intensity of monoclinic phase ZrO_2 (Baddeleyite) appeared in XRD patterns of all the materials except SZr-Ti-Yb-500-4/s. This evidenced the better selectivity and activity performances influenced by the high S_{BET}, which reflects small crystallite size. However, monoclinic phase was more prominent on SZr-500-4/10 than for others (Fig. 2a) though with minimal effect.

3.2. BET analysis

Table 2 presents the textural properties and acidity of the mesoporous SZ catalysts. The difference in chemical composition of the catalytic materials plausibly explains the significant variations in textural and catalytic activities. Thus, for instance, the S_{BET} of SZr-500-5/10 was 15.0543 m^2/g while SZr-500-5/7 had 7.6917 S_{BET} value. However, the pore size distribution ($2 < d_p < 50$ nm) of all the synthesized catalysts revealed mesoporous structure which permits the TG molecule access to the active sites within the materials (Table 2, Fig. 3).

Figs. 3a and b show nitrogen sorption isotherms of the SZ obtained after calcination in air at 500 °C. The isotherms followed the type III of the IUPAC classification with pores in the range of 1.5–100 nm. This indicates the mesoporous nature of the synthesized materials, which are typical of nonporous materials with weak fluid-wall attractive forces. The slopes show increased adsorbate uptake at higher pressures as the gas fills the pores, while inflection point occurs typically near completion of the first monolayer. Expectedly, the voids between the zirconia nanocrystals showed a H_2 type hysteresis loop befitting of inkbottle pores. The isotherms of SZr-500-5/7, SZr-500-5/7R, SZr-500-5/10, and SZr-500-5/14 shifted to higher adsorbed volumes with increasing aging and pH. This indicated increase in specific surface area, S_{BET} of the materials (Table 2). For instance, the S_{BET} for the materials aged for 7, 10, and 14 days produced 9, 15, and 41 m^2/g, respectively. This corroborated the report by Cassiers et al. [21] that large specific surface area needs higher post-treatment of *ca.* pH 12.

Intriguingly, the study obtained inverse correlations from the pore size distributions (Figs. 4a and b) which shifted to smaller diameters with increasing aging and pH (Table 2). Materials aged for 7 days (pH 1.25) produced about 21 nm, against 7 nm for materials aged for 14 days (pH 5). Interestingly, impregnating 5 wt. % titanium into the zirconium hydroxide had a pronounced effect on the S_{BET} of the SZ. However, this modification had negligible effect on the pore size distribution of the calcined materials (Table 2; Fig. 4a, and b). Similar shifts were observed in the pore size distributions and the isotherms from both Ti-free materials and those impregnated with titania.

To further evaluate the effect of incorporating transition-metal on the structural and acidic properties on activity of SZ, 1.5 wt. % ytterbium (III) nitrate hydrate was used in preparing SZr-Ti-Yb-500-4/s. The corresponding material exhibited the highest S_{BET} of 60 m^2/g and a high pore size distribution (21 nm) comparable to the other materials (Fig. 5). Further, this SZ exhibited the highest acidity of 33×10^{-2} mmol/g. These observations suggest that longer aging period of the precipitating agent within aggregates of nanocrystals in the interparticle voids leads to higher S_{BET} and lower crystal size. The pore system of the resulting material was significantly higher than the samples without Yb; whereas at relative pressures < 0.8, the nitrogen sorption isotherm remained similar (Figs. 3 to 5). The higher sorption capacity of SZ doped with Yb at higher relative pressures confirmed the existence of mesopores with a broad size distribution. Similarly, this is evident from the pore size distribution (Fig. 5) which instead of the expected 3–8 nm, revealed a broad distribution of mesopores of 3–60 nm. The authors attributed this observation to volumes between the interparticle voids and nanocrystal aggregates. Consequently, Yb incorporation narrows the pore size distribution because of even crystal size distribution and even Zr aggregate size (Fig. 5). An earlier study by Cassiers et al. [21] showed the effect that scaffolding DDA support has on mesoscale of zirconia.

3.3. Ammonia temperature-programmed desorption

Impregnating zirconium with Ti and Yb as described above aimed at synthesizing catalytically active materials. The acid strength of

Please cite this article as: Y.M. Sani et al., Acidity and catalytic performance of Yb-doped SO_4^{2-}/Zr in comparison with SO_4^{2-}/Zr catalysts synthesized *via* different preparatory conditions for biodiesel production, Journal of the Taiwan Institute of Chemical Engineers (2015), http://dx.doi.org/10.1016/j.jtice.2015.07.016

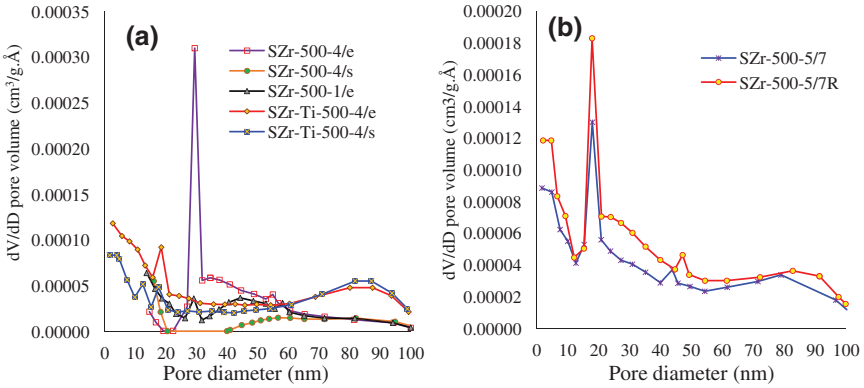

Fig. 4. Pore size distribution curves of mesoporous SZ prepared from different preparatory conditions.

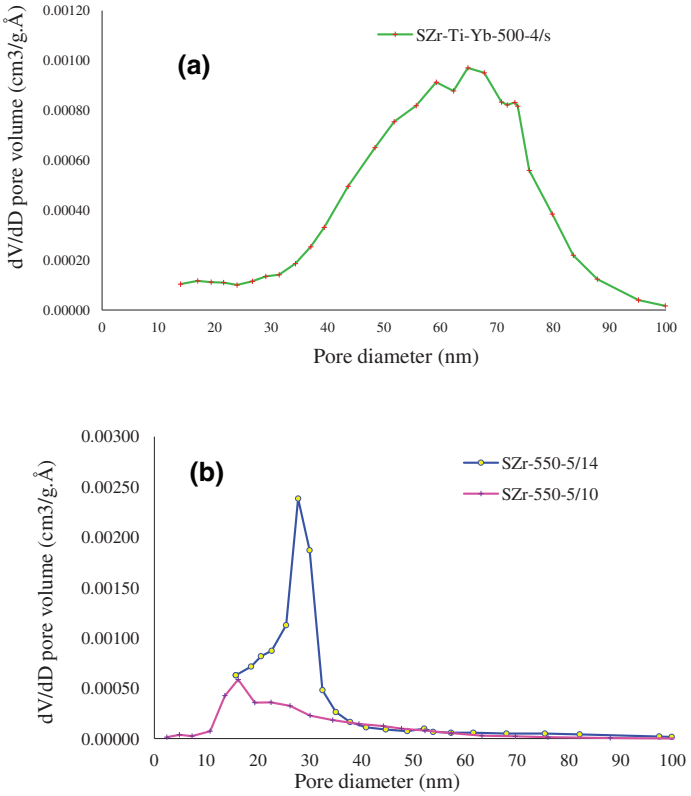

Fig. 5. Pore size distribution curves of mesoporous SZ prepared from different preparatory conditions.

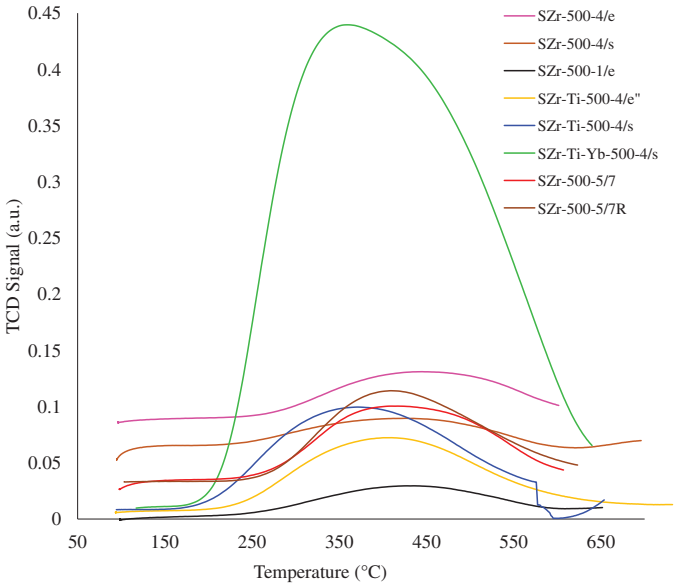

Fig. 6. NH_3-temperature-programmed desorption profiles for the synthesized catalysts.

the SZ was experimentally investigated by temperature-programmed ammonia desorption (NH_3-TPD). Fig. 6 shows representative NH_3-TPD profiles of some of the SZ calcined at 500 °C. A low-temperature desorption peak with a maximum around 400 °C was detected. Except for SZr-Ti-Yb-500-4/s, the NH_3-TPD thermograms revealed flat and broad NH_3 desorption peaks. This indicates the presence of strong acid sites distribution on the synthesized catalysts. The shapes of the NH3-TPD profiles were consistent with those reported for comparable mesoporous zirconium titanium oxide nanospheres reported by [22–24]. All synthesized materials except SZr-Ti-Yb-500-4/s, exhibited predominantly weak Lewis acids property [25,26] because Brønsted sites are desorbed at temperatures higher than 400 °C [27,28]. These authors assigned broad peaks at temperatures below 600 °C as a conglomerate of overlapping component peaks. The peaks may include ammonia desorption from bound strong Lewis acid sites, NH_4^+ ions decomposition and those released from weak Lewis acid sites. The latter desorption may also include coordinately unsaturated titanium and zirconium ions. We assigned the low-temperature desorption of the bulk titanium oxide to the weak support interaction, which corroborated the report by [29]. However, SZr-Ti-Yb-500-4/s generated strong Lewis and Brønsted acidity from its sulfate groups (Fig. 6). Evidently, this material possessed more acid sites than the other materials because of its available protons for donation. Table 2 presents the strength of the acid sites calculated from the ammonia thermodesorption curves.

A notable increase in the number of acid sites was observed in the Zr–Ti mixed oxide catalysts compared to SZ without titania. This is despite the shorter aging period of the former (15 min) against the latter (120 min). These observations are in complete accordance with previous reports [30] that mixed oxides generate more acid sites than single oxides. One of two mechanisms premised this hypothesis: (a) zirconium atoms substituting some of the titanium atoms or (b) large dispersion effect on the surface of the mixed oxide by the ZrO_2 or TiO_2. To investigate the activity of the surface acid sites on the SZ further, see discussion on the catalytic results section. Simultaneous esterification of FFA and transesterification of TG validated the acid catalytic activity of the synthesized SZ. Fig. 7a illustrates the surface microstructure of SZr-500-4/e as studied using FESEM, showing solid particles of uniform dimensions homogeneously processed from

Please cite this article as: Y.M. Sani et al., Acidity and catalytic performance of Yb-doped SO_4^{2-}/Zr in comparison with SO_4^{2-}/Zr catalysts synthesized *via* different preparatory conditions for biodiesel production, Journal of the Taiwan Institute of Chemical Engineers (2015), http://dx.doi.org/10.1016/j.jtice.2015.07.016

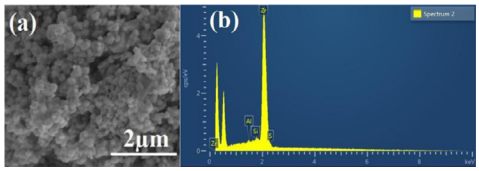

Fig. 7. (a) Results of the surface microstructural analysis of the SZr-500-4/e via FE-SEM and (b) surface elemental composition of the SZr-500-4/e determined via EDX analysis.

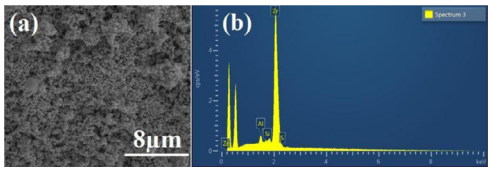

Fig. 8. (a) Results of the surface microstructural analysis of the SZr-500-4/s via SEM and (b) surficial elemental composition of the SZr-500-4/s via EDX analysis.

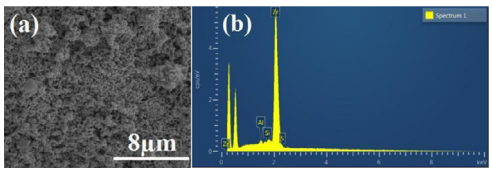

Fig. 9. (a) Results of the surface microstructural analysis of the SZr-500-1/e (15 min) via SEM and (b) surficial elemental composition of the SZr-500-1/e (15 min) via EDX analysis.

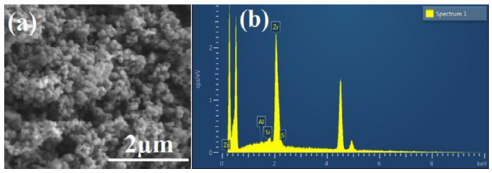

Fig. 10. (a) Results of the surface microstructural analysis of the SZr-Ti-500/e (15 min) via SEM and (b) surficial elemental composition of the SZr-Ti-500/e via EDX analysis.

different constituents. The EDX analysis of the surface elemental composition revealed the presence of zirconium (99.63 wt. %) and sulfur (0.16 wt. %) (Fig. 7b).

Similarly, Fig. 8(a) presents the surface microstructure (size and shape of topographic features) of sulfonated SZr-500-4/s catalyst studied using FE-SEM. The surface morphology has been homogeneously processed into solid particles. The surficial elemental composition by EDX analysis (Fig. 8b) also revealed the presence of 98.14 wt. % zirconium and 0.10 wt. % sulfur. The surficial appearance of SZr-500-4/e revealed a lesser dispersion of surface elements than SZr-500-4/s. Interestingly, the acid site density of the latter was also higher than that of the former. However, the catalyst calcined for 1 h (SZr-500-1/e) revealed a similar surficial micrograph (Fig. 9).

Fig. 10(a) presents the surface microstructure (size and shape of topographic features) of SZr-Ti-500/e catalyst. Calcination incorporated and stabilized the titanium oxide into crystal lattices of zirconium oxide structure. Fig. 10(b) presents a cross-sectional surficial composition and distribution of elements on SZr-Ti-500/e via EDX analysis. However, the micrograph of the catalyst prepared with sufficient acid revealed a more dispersed surficial metal elements (Fig. 11a). Expectedly, micrograph representing SZr-Ti-Yb-500-4/s (Fig. 12a) displayed a somewhat amorphous phase.

As expected, the differences between the micrographs of SZr-500-5/7 (Fig. 13a) and SZr-500-5/7R (Fig. 14a) were hardly noticeable. Intriguingly however, the surficial structures of SZr-500-4/14 and that of SZr-500-5/10 (Fig. 15a) were markedly dissimilar.

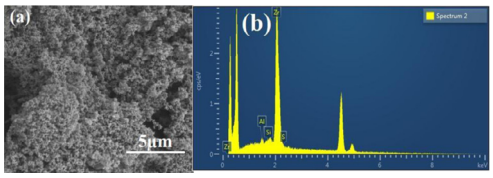

Fig. 11. (a) Results of the surface microstructural analysis of the SZr-Ti-500-4/s (15 min) via SEM and (b) surficial elemental composition of the SZr-Ti-500-4/s via EDX analysis.

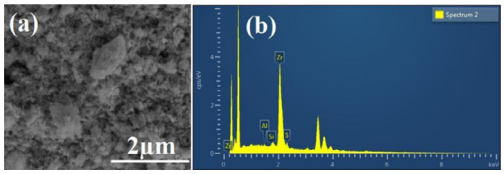

Fig. 12. (a) Results of the surface microstructural analysis of the SZr-Ti-Yb-500-4/s via SEM and (b) surficial elemental composition of the SZr-Ti-Yb-500-4/s via EDX analysis.

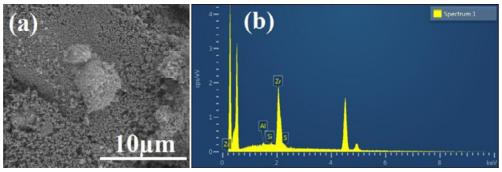

Fig. 13. (a) Results of the surface microstructural analysis of the SZr-500-5/7 via SEM and (b) surficial elemental composition of the SZr-500-5/7 via EDX analysis.

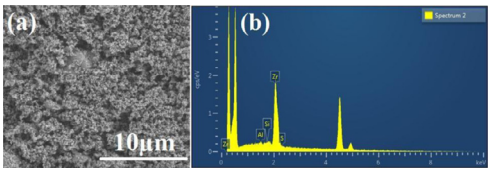

Fig. 14. (a) Results of the surface microstructural analysis of the SZr-500-5/7R via SEM and (b) surficial elemental composition of the SZr-500-5/7R via EDX analysis.

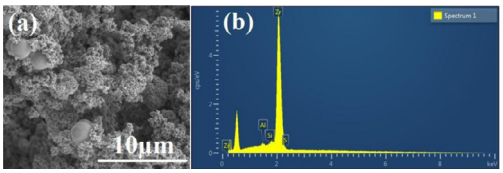

Fig. 15. (a) Results of the surface microstructural analysis of the SZr-500-5/10 via SEM and (b) surficial elemental composition of the SZr-500-5/10 via EDX analysis.

4. Acid activity of mesoporous SZ catalysts

It is also instructive to note that impregnating sulfate onto zirconium oxide produces acidic solid catalysts. The high conversions displayed by the synthesized materials reflect the role of this incorporation. This is despite the moderate S_{BET} values of the synthesized catalytic materials (Table 2). The study attributed acidity of the SZ to the SO_4^{2-} ions on surface acid sites of the materials. This further affirmed the presence of sulfate active sites within the surface structure of the catalysts as reported by [31]. However, it is instructive to note that zirconia support provided the essential acid site [32]. It is therefore plausible to assert that acidity of materials synthesized in this study have direct correlation to surface hydroxyl groups. Soaking for the same period (15 min) in excess 0.5-M H_2SO_4 led to a decrease in acidity from (70 to 50) x 10^{-3} mmol/g and average pore diameter from about 29 to 25 nm.

Please cite this article as: Y.M. Sani et al., Acidity and catalytic performance of Yb-doped SO_4^{2-}/Zr in comparison with SO_4^{2-}/Zr catalysts synthesized *via* different preparatory conditions for biodiesel production, Journal of the Taiwan Institute of Chemical Engineers (2015), http://dx.doi.org/10.1016/j.jtice.2015.07.016

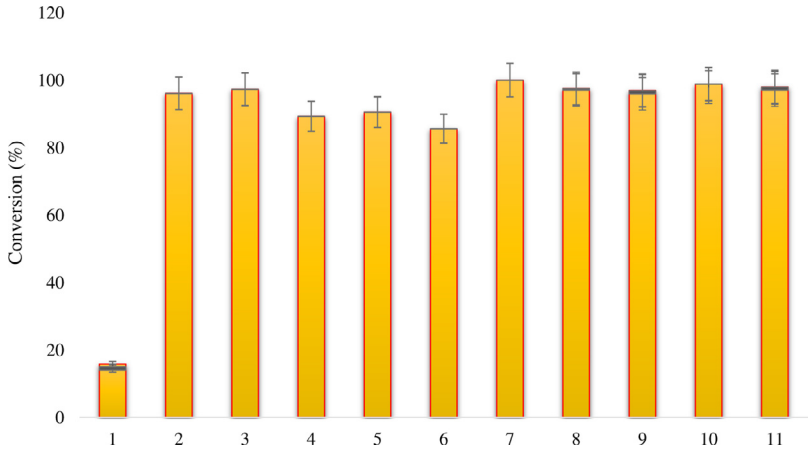

Fig. 16. Different mesoporous SZ catalysts employed at 200 °C for 5 h (1 = unsulfated Zr; 2 = SZr-500-4/e; 3 = SZr-500-4/s; 4 = SZr-500-1/e; 5 = SZr-Ti-500-4/e; 6 = SZr-Ti-500-4/s; 7 = SZr-Ti-Yb-500-4/s; 8 = SZr-500-5/7; 9 = SZr-500-5/7R, 10 = Zr-500-5/14, 11 = SZr-500-5/10).

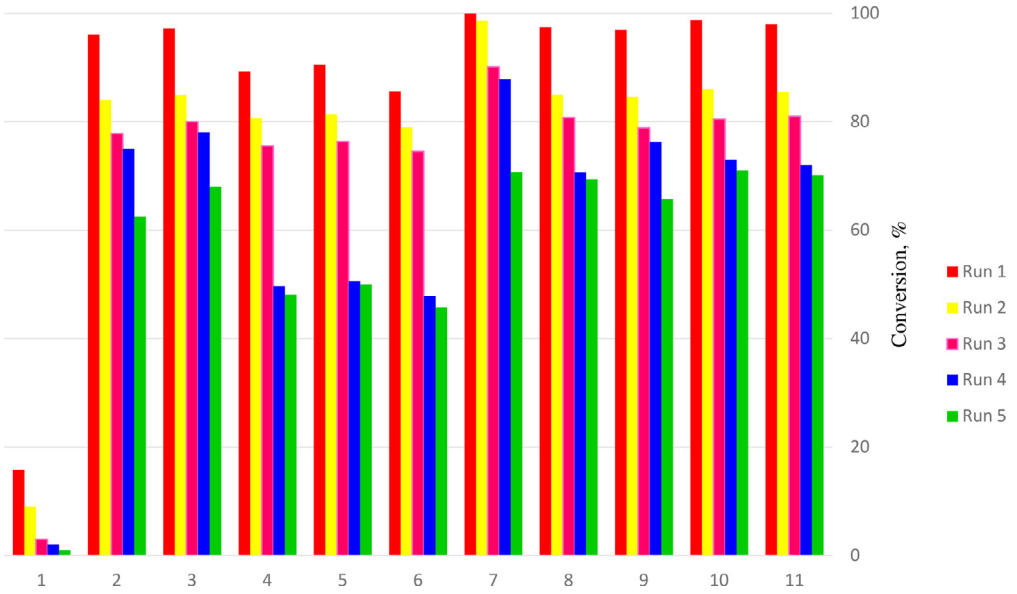

Fig. 17. Performance of regenerated SZ catalysts employed at 200 °C for 5 h (1 = unsulfated Zr; 2 = SZr-500-4/e; 3 = SZr-500-4/s; 4 = SZr-500-1/e; 5 = SZr-Ti/500-4/e; 6 = SZr-Ti-500-4/s; 7 = SZr-Ti-Yb-500-4/s; 8 = SZr-500-5/7; 9 = SZr-500-5/7R, 10 = Zr-500-5/14, 11 = SZr-500-5/10).

However, the S_{BET} remained essentially unaffected at 8.33 m^2/g for sample (SZr-Ti-500-4/e) prepared in excess acid and 8.12 m^2/g for SZr-Ti-500-4/s synthesized in sufficient 0.5-M H_2SO_4. Similarly, both materials exhibited negligible change in pore volumes (Table 2). Expectedly, a TG molecule requires a critical diameter or the smallest access cylinder of 2–4 nm [33,34]. Srilatha et al. [35] reported severe internal diffusion resistance. However, Lopez et al. [36] obtained 57% conversion from SZ with S_{BET} of 134.4 ± 5.3 m^2/g. Premised on the underlying difficulty of TG molecules to access inner pores of the catalysts, it is plausible to assert that amount, and dispersion of active sites that is reflective of acidity is responsible for transesterification activity reported in this study. Furthermore, variation in titanium loading by an order of magnitude did not have significant effect on the acid site density. These findings agreed with those reported by Viinikainen et al. [32]. Incidentally, S_{BET} increases with aging period (Table 2, Fig. 3). This ensures consequent stabilization and high dispersion of the nano-particles into tetragonal phase. Hence, the observed lower sintering and coking from the catalysts despite their low specific surface area.

Though all the samples exhibited good performances when evaluated for transesterification of used frying oil (Fig. 16), SZr-Ti-Yb-500-4/s displayed higher activity compared to the others. For instance, SZr-Ti-Yb-500-4/s, SZr-500-5/14, SZr-500-5/10, and SZr-500-5/7 gave a yield of 91%, 85%, 77%, and 76%, respectively. We ascribed this to its superior acidity (Fig. 6). Further, interaction between the tetragonal phase of the zirconia support (facilitated by highly dispersed nanoparticles) and higher mesopores determines the acidity and activity of the SZ. We ascribed the high acid-catalyzed activity of the other catalysts to a combination of acidity and the dominant presence of tetragonal phase as shown by the XRD patterns. This indicates that monoclinic phase does not favor transesterification of UFO as much as tetragonal phase of the evaluated materials. This is in consonance with the report of Ramu et al. [37].

Interestingly, the presence of ytterbium facilitated higher specific surface area and acidic sites on the catalysts. However, loading titanium onto zirconia decreases the density of the surface acid sites. Thus, the activity of SZr-Ti-500-1/e, SZr-Ti-500-4/e, and SZr-Ti-500-4/s were comparatively lower than were obtainable from the other catalysts. The difference in chemical composition of the catalytic materials plausibly explains the significant variations in textural and catalytic activities. Incidentally, SZr-Ti-500-1/e displayed the lowest acid density. Thus, for instance, the S_{BET} of SZr-500-5/10 was 15.05 m^2/g

Please cite this article as: Y.M. Sani et al., Acidity and catalytic performance of Yb-doped SO_4^{2-}/Zr in comparison with SO_4^{2-}/Zr catalysts synthesized *via* different preparatory conditions for biodiesel production, Journal of the Taiwan Institute of Chemical Engineers (2015), http://dx.doi.org/10.1016/j.jtice.2015.07.016

(97.98% conversion) while SZr-500-1/e with 3.84 m^2/g S_{BET} value had a lower conversion of 85.55%. The catalysts were regenerated by decantation, methanol washing, drying, and calcining. Expectedly, compared to the others the catalyst, SZr-Ti-Yb-500-4/s retained most of its activity and displayed better performance after 5 recycles (Fig. 17). Evidently, Yb-doped SZ ensured the high stability, and good reusability of the synthesized catalyst. This is despite the presence of Ti, which decreases the surface acid sites density. However, as the surface loses its sulfate ions after several cycles, deactivation sets in on the materials.

Transforming feedstocks of low economic value into high yield FAMEs with increased desired product selectivity, and enhanced recycling and reusability opportunities demonstrate the advantage of solid acid catalysts. Incidentally, the strategy of doping SZ with Yb proves economical. It employed moderate reaction conditions such as relatively low catalyst loading, and a 5:1 alcohol-to-oil ratio to convert more than 99% high FFA feedstock. This is interesting when compared with other SZ solid acid catalysts employed under similar condition and feedstock. For instance, Park et al. [38] obtained 70% conversion with WO_3/ZrO_2 (S_{BET} = 40 m^2/g; pore size = 11 nm). Despite the high S_{BET} of 258 m^2/g, Peng et al. [39], achieved 90% conversion with SZr-Ti-Si. This was achieved with a 9:1 methanol-to-oil molar ratio at 200 °C for 4 h and a catalyst loading of 3 wt. %. Conversely, it is noteworthy to mention the result by Feng et al. [40]. The authors achieved 90% conversion cation exchange resin (S_{BET} = 77 m^2/g; pore size = 56 nm) under a low temperature of 64 °C from FFA-containing feedstock. However, the study employed 20 wt. % catalyst after 4 h and 6:1 methanol-to-oil molar ratio.

5. Conclusion

In summary, this study demonstrated a facile route for synthesizing efficient solid acid catalysts for transesterifying UFO. Doping SZ with ytterbium is a key feature of this synthesis strategy. The process stabilizes the mesostructured channels and crystallographic phase, and produces high amount and good dispersion of the active sites that ensures higher catalytic performance. The excellent results obtained from this study highlight the need for further research in this area. Other significant findings include: (1) slight modification in catalyst preparation condition yields different catalytic activity. Such modifications affected the domain size and lattice strain of the material. (2) The observed low specific surface area was probably due to shorter precipitating period. However, the encouraging conversions obtained suggest that activity for transesterification does not depend solely on textural property of the catalytic material. (3) Amount and dispersion of active sites, which are reflective of acidity of SZ, play significant role in facilitating higher conversion of TG into biodiesel. (4) The study also showed how to achieve a flexibility of properties from unlimited number of possible manipulations from one catalyst precursor. These observations highlight the possibility of improving on the reported formulations to facilitate higher intrinsic efficiency in biodiesel production.

Acknowledgment

This study was carried out with the aid of research grants from Fundamental Research Grant Scheme, FRGS (Project No: FP031-2013A) under University of Malaya and Tertiary Education Trust Fund (TETFund), Ahmadu Bello University, Zaria Nigeria.

Supplementary materials

Supplementary material associated with this article can be found, in the online version, at doi:10.1016/j.jtice.2015.07.016.

References

[1] Sani YM, Daud WMAW, Abdul Aziz AR. Activity of solid acid catalysts for biodiesel production: a critical review. Appl Catal A 2014;470:140–61.
[2] Sani YM, Daud WMAW, Abdul Aziz AR. Solid acid-catalyzed biodiesel production from microalgal oil: the dual advantage. J Environ Chem Eng. 2013;1:113–21.
[3] Reddy C, Reddy V, Oshel R, Verkade JG. Room-temperature conversion of soybean oil and poultry fat to biodiesel catalyzed by nanocrystalline calcium oxides. Energy Fuels 2006;20:1310.
[4] Garcia CM, Teixeira S, Marciniuk LL, Schuchardt U. Transesterification of soybean oil catalyzed by sulfated zirconia. Bioresour Technol. 2008;99:6608–13.
[5] Hino M, Kobayashi S, Arata K. Solid catalyst treated with anion. 2. Reactions of butane and isobutane catalyzed by zirconium oxide treated with sulfate ion: solid superacid catalyst. J Am Chem Soc. 1979;101:6439–41.
[6] Morterra C, Cerrato G, Bolis V, Di Ciero S, Signoretto MJ. On the strength of Lewis- and Brønsted-acid sites at the surface of sulfated zirconia catalysts. Chem Soc Faraday Trans. 1997;93:1179–84.
[7] Drago R, Kob N. Acidity and reactivity of sulfated zirconia and metal-doped sulfated zirconia. J Phys Chem B 1997;101:3360–4.
[8] Adeeva V, de Haan JW, Jänchen J, Lei GD, Schünemann V, van de Ven LJM, et al. Acid sites in sulfated and metal-promoted zirconium dioxide catalysts. J Catal. 1995;151:364–72.
[9] Haase F, Sauer J. The surface structure of sulfated zirconia: periodic ab initio study of sulfuric acid adsorbed on ZrO_2 (101) and ZrO_2 (001). J Am Chem Soc. 1998;120:13503–12.
[10] Yamaguchi T, Jin T, Tanabe K. Structure of acid sites on sulfur-promoted iron oxide. J Phys Chem. 1986;90:3148–52.
[11] Jin T, Yamaguchi T, Tanabe KJ. Mechanism of acidity generation on sulfur-promoted metal oxides. Phys Chem. 1986;90:4794–6.
[12] Morterra C, Cerrato G, Pinna F, Signoreto M. Crystal phase, spectral features, and catalytic activity of sulfate-doped zirconia systems. J Catal. 1995;157:109–23.
[13] Hassan S.N., Sani Y.M., Abdul Aziz A.R., Sulaiman N.M.N., Daud W.M.A.W. Biogasoline: an out of-the-box solution to the food-for-fuel and land-use competitions. 2015;89:349-367.
[14] Haigh KF, Vladisavljević GT, Reynolds JC, Nagy Z, Saha B. Kinetics of the pretreatment of used cooking oil using Novozyme 435 for biodiesel production. Chem Eng Res Des. 2014;92:713–19.
[15] Suharto TE. Synthesis of catalytically active high surface area sulfated zirconia. J Math Sains 2003;8:171–3.
[16] Osendi MI, Moya JS, Serna CJ, Soria J. Metastability of tetragonal zirconia powders. J Am Ceram Soc. 1985;68:135–9.
[17] Tangchupong N, Khaodee W, Jongsomjit B, Laosiripojana N, Praserthdam P, Assabumrungrat S. Effect of calcination temperature on characteristics of sulfated zirconia and its application as catalyst for isosynthesis. Fuel Proc Technol. 2010;91:121–6.
[18] Fărcaşiu D, Li JQ, Cameron S. Preparation of sulfated zirconia catalysts with improved control of sulfur content II: effect sulfur of sulfur content on physical properties and catalytic activity. Appl Catal A 1997;154:173–84.
[19] Vishwanathan V, Balakrishna G, Rajesh B, Jayasri V, Sikhwivhilu LM, Coville NJ. Alkylation of catechol with methanol to give guaiacol over sulphate-modified zirconia solid acid catalysts: the influence of structural modification of zirconia on catalytic performance. Catal Commun. 2000;9:2422–7.
[20] Pacheco G, Fripiat JJ. Physical chemistry of the thermal transformation of mesoporous and microporous zirconia. J Phys Chem B 2000;104:11906–11.
[21] Cassiers K, Linssen T, Aerts K, Cool P, Lebedev O, Van Tendeloo G, et al. Controlled formation of amine-templated mesostructured zirconia with remarkably high thermal stability. J Mater Chem. 2003;13:3033–9.
[22] Rezaei M, Alavi SM, Sahebdelfar S, Bai P, Liu XM, Yan ZF. CO_2 reforming of CH_4 over nanocrystalline zirconia-supported nickel catalysts. Appl Catal B 2008;77:346–54.
[23] Rezaei M, Alavi SM, Sahebdelfar S, Qian L, Yan Z-F. CO_2-CH_4 reforming over nickel catalysts supported on mesoporous nanocrystalline zirconia with high surface area. Energy Fuels 2007;21:581–9.
[24] Guan B, Wang T, Zeng S, Wang X, An D, Wang D, et al. A versatile cooperative template-directed coating method to synthesize hollow and yolk-shell mesoporous zirconium titanium oxide nanospheres as catalytic reactors. Nano Res. 2013;7:246–62.
[25] Barthos R, Lónyi F, Onyestyák G, Valyon J. An IR, FR, and TPD study on the acidity of H-ZSM5, sulfated zirconia, and sulfated zirconia-titania using ammonia as the probe molecule. J Phys Chem B 2000;104:7311–19.
[26] Lónyi F, Valyon J, Engelhardt J, Mizukami F. Characterization and catalytic properties of sulfated ZrO_2-TiO_2 mixed oxides. J Catal. 1996;160:279–89.
[27] Zou H, Lin YS. Structural and surface chemical properties of Sol-Gel derived TiO_2-ZrO_2 oxides. Appl Catal A 2004;265:35–42.
[28] Das D, Mishra HK, Dalai AK, Parida KM. Isopropylation of benzene over sulfated ZrO_2-TiO_2 mixed-oxide catalyst. Appl Catal A 2003;243:271–84.
[29] Mile B, Stirling D, Zammitt MA, Lovell A, Webb M. TPR studies of the effects of preparation conditions on supported nickel catalysts. J Mol Catal. 1990;62:179–98.
[30] Manríquez ME, López T, Gómez R, Navarrete J. Preparation of TiO_2-ZrO_2 mixed oxides with controlled acid-basic properties. J Mol Catal A Chem. 2004;220:229–37.
[31] Hino M, Kurashige M, Matsuhashi H, Arata K. The surface structure of sulfated zirconia: studies of XPS and thermal analysis. Thermochimica 2006;441:35–41.

Please cite this article as: Y.M. Sani et al., Acidity and catalytic performance of Yb-doped SO_4^{2-}/Zr in comparison with SO_4^{2-}/Zr catalysts synthesized *via* different preparatory conditions for biodiesel production, Journal of the Taiwan Institute of Chemical Engineers (2015), http://dx.doi.org/10.1016/j.jtice.2015.07.016

[32] Viinikainen T, Rçnkkçnen H, Bradshaw H, Stephenson H, Airaksinen S, Reinikainen M, et al. Krause, acidic and basic surface sites of zirconia-based biomass gasification gas clean-up catalysts. Appl Catal A 2009;362:169–77.
[33] Fernandez MB, Tonetto GM, Crapiste G, Damiani DE. Kinetics of the hydrogenation of sunflower oil over alumina supported palladium catalyst. Int J Chem React Eng. 2007;5:10.
[34] Kiss AA, Dimian AC, Rothenberg G. Solid acid catalysts for biodiesel production-towards sustainable energy. Adv Synth Catal. 2006;348:75–81.
[35] Srilatha K, Kumar ChR, Prabhavathi Devi BLA, Prasad RBN, Sai Prasad PS, Lingaiah N. Efficient solid acid catalysts for esterification of free fatty acids with methanol for the production of biodiesel. Catal Sci Technol. 2011;1:662–8.
[36] López DE, Goodwin JG Jr, Bruce DA, Lotero E. Transesterification of triacetin with methanol on solid acid and base catalysts. Appl Catal A 2005;295:97–105.
[37] Ramu S, Lingaiah N, Prabhavathi Devi BLA, Prasad RBN, Suryanarayana I, Sai Prasad PS. Esterification of palmitic acid with methanol over tungsten oxide supported on zirconia solid acid catalysts: effect of method of preparation of the catalyst on its structural stability and reactivity. Appl Catal A 2004;276:163–8.
[38] Park YM, Lee DW, Kim DK, Lee JS, Lee KY. The heterogeneous catalyst system for the continuous conversion of free fatty acids in used vegetable oils for the production of biodiesel. Catal Today 2008;131:238–43.
[39] Peng BX, Shu Q, Wang JF, Wang GR, Wang DZ, Han MH. Biodiesel production from waste oil feedstocks by solid acid catalysis. Proc Safety Environ Protect. 2008;86:441–7.
[40] Feng Y, He B, Cao Y, Li J, Liu M, Yan F, et al. Biodiesel production using cation-exchange resin as heterogeneous catalyst. Bioresour Technol. 2010;101:1518–21.

Please cite this article as: Y.M. Sani et al., Acidity and catalytic performance of Yb-doped SO_4^{2-}/Zr in comparison with SO_4^{2-}/Zr catalysts synthesized *via* different preparatory conditions for biodiesel production, Journal of the Taiwan Institute of Chemical Engineers (2015), http://dx.doi.org/10.1016/j.jtice.2015.07.016